# New Geant4 photonuclear cross-section model

*Student: Bogdan Kutsenko[1], bdkutsenko@gmail.com*
*Supervisor: Vladimir Ivantchenko[2]*

CERN summer student program 2021

[1] Novosibirsk State University, Novosibirsk, Russia
[2] CERN, Geneva, Switzerland

**Abstract**

A new photonuclear cross-section model for the Geant4 toolkit is presented. The model is based on IAEA evaluated photonuclear data library at giant dipole resonance energy region from 0 MeV to 130 MeV. Description of processing algorithm of IAEA ENDFL-6 data files to the Geant4 database is provided. Overview of the new class and comparison of the model cross-section output with experimental data and the previous implementation of photonuclear cross-sections of Geant4 is presented. The new model will be publicly available with Geant4 11.0.

**Keywords**

GEANT4; Photonuclear; Cross-section; IAEA; Database;

# Contents

# 1 Introduction

At low energies a photonuclear interaction begins with the absorption of a photon by a nucleus, leaving the nucleus in an excited state. The excited nucleus then undergoes the de-excitation process, emitting secondary particles and possibly undergoing fission. At high energies photon may produce nuclear resonances and strings.

Photons are commonly produced as bremsstrahlung radiation by electron accelerators, which are presented at many laboratories, industries and hospitals. Even though nowhere on an energy scale below the $10^{20}$ eV photo-nuclear cross-section surpasses pair production cross-section, the interaction between photon and nuclei plays a significant role in the high energy electromagnetic showers. For a large number of photons with energies close to the giant dipole resonance, a large number of neutrons can be produced, influencing the transverse distribution of an electromagnetic shower. At very high energies, photon pair production cross-sections are heavily suppressed by the Landau–Pomeranchuk–Migdal effect, and photo-nuclear interactions predominate over electromagnetic interactions [1].

The application of photo-nuclear interaction is not limited to the correction of the elementary particle detector response simulation of a photon passing through matter. Other possible application includes but not limited to: calculation of absorbed doses in the human body, radiation shielding and radiation transport analyses, activation analyses, nuclear waste transmutation, fission reactor technologies, plasma diagnostics, astrophysical nucleosynthesis.

# 2 Photonuclear absorption

Theoretical prediction of a photonuclear cross-section is not possible due to the complexity of this process. Therefore the cross-section should be based on data.

## 2.1 Experimental data

To determine the photonuclear absorption cross-section it is necessary to measure the flux of incident photons and the number of the emitted particles. The measurement of the photon flux can be done with scintillators, solid-state detectors, or an ionization chamber. Furthermore, the amount of emitted particles measurement can be done either directly using drift chamber and calorimeter, or by counting activity of the residual nuclei if it is unstable. One of the main problems in experimental studies of photo-nuclear absorption reactions is the intense source of monoenergetic photons, there are several methods exist to solve this problem:

- Generate continuous bremsstrahlung radiation produced by an electron beam hitting a radiator target [2];
- Produce quasi mono-energetic beams by either relativistic positron annihilation or laser Compton scattering [3, 4].

In the case of bremsstrahlung radiation photonuclear cross-section derived by either unfolding procedure of the observed data [5], or using a thin radiator and photon tagging. Photon tagging is carried out through the selection of electrons from the beam that hit a thin radiator target with energy within the acceptance range of the spectrometer. The selection of electrons is performed using a magnetic field.

The resulting spectral distribution of photons can differ in shape, average energies, and absolute values depending on the method used to obtain a quasi mono-energetic beam. The discrepancies in total photonuclear cross-section from the different experiments were analyzed, and it was shown that evaluation data is needed [6]. In 2019 the recent report of photonuclear reactions became available [7].

### 2.2 Cross-section energy regions

At the lowest energies of the incident photon only scattering from the nuclear charge, or Thomson scattering can take place. At slightly higher energies $\backsim$1-200 MeV photon can excite nuclear energy levels and be absorbed by a nucleus through two distinct reaction mechanisms [8] :

- Giant Dipole Resonance (GDR);
- Quasi-deuteron (QD) photoabsorption.

GDR is the large maximum in the cross-section and dominant feature of the photoabsorption process for nuclei. GDR peak in the photo-absorption cross-section was interpreted by Goldhaber and Teller [9] as the excitation of a collective nuclear vibration in which all the protons in the nucleus move collectively against all the neutrons providing a separation between the centers of mass and charge, thus creating an electric dipole moment. Therefore GDR is attributed primarily to electric dipole absorption for an incident photon with energy ($E_\gamma = 10 - 20\ MeV$). Furthermore, it can be seen in all nuclei and may be viewed as a general property of nuclear matter. Experimental data show isolated resonance like structures [10] which can be represented most suitably and simply with a Breit–Wigner shape:

$$\sigma_{gdr}(E_\gamma) = \sigma_R \frac{E_\gamma^2 \Gamma_R^2}{(E_R^2 - E_\gamma^2)^2 + E_\gamma^2 \Gamma_R^2} \ , \tag{1}$$

where $\sigma_R$, $E_R$ and $\Gamma_R$ are the resonance peak cross-section, energy, and width respectively. This approximation can be too simple in the case of deformed nuclei or light nuclei. In the deformed nuclei the photo-absorption cross-section is given by the sum of two giant dipole resonances and described by the standard Lorentzian parameterization (SLO). SLO can reasonably well describe GDR around the peak, but it can show significant discrepancies with the experimental data around the neutron separation energy ($\backsim 2 - 10\ MeV$). Because of these discrepancies, Simple Modified Lorentzian (SMLO) [11] were developed and used more commonly in photonuclear cross-section parameterization around the GDR energy region. The other problem is connected with light nuclei, where quadruple oscillations of the nuclear surface can modify cross-section form significantly. Therefore for the light nuclear model cross-section evaluation, a more complex approach should be implemented with a very detailed structure of the individual nuclei energy levels.

The QD component is related to the experimental deuteron photodisintegration cross-section as following:

$$\sigma_{qd}(E_\gamma) = L \sigma_d(E_\gamma) f(E_\gamma) \frac{NZ}{A} \ , \tag{2}$$

where L = 6.5 is the Levinger parameter taken from the Chadwick model [12], N - number of neutrons, Z - number of protons, A - atomic number, and $f(E_\gamma)$ - Pauli-blocking function of the excited neutron and proton which also derived from Chadwick model at the energy region between $20 - 140\ MeV$.

For higher energies, after GDR and QD regions ($\backsim 150\ MeV$) delta and photo-meson resonances are following as presented in Figure 1. Delta resonance has a threshold that is associated with pion mass and the process kinematic - ($E_\gamma > 140\ MeV$) and correspond to pion production that can take place through two different reactions:

$$\sigma(\gamma + p \to p + \pi^0) = \sigma(\gamma + n \to n + \pi^0) \tag{3}$$

$$\sigma(\gamma + p \to n + \pi^+) = \sigma(\gamma + n \to p + \pi^-) \tag{4}$$

Photo-meson energy region corresponds to other delta baryons ($\Delta^0, \Delta^{++}, \Delta^+, \Delta^-$) resonances.

At still higher energies cross-section continue to increase according to Froissart bound $ln^2(s)$ approximation [1].

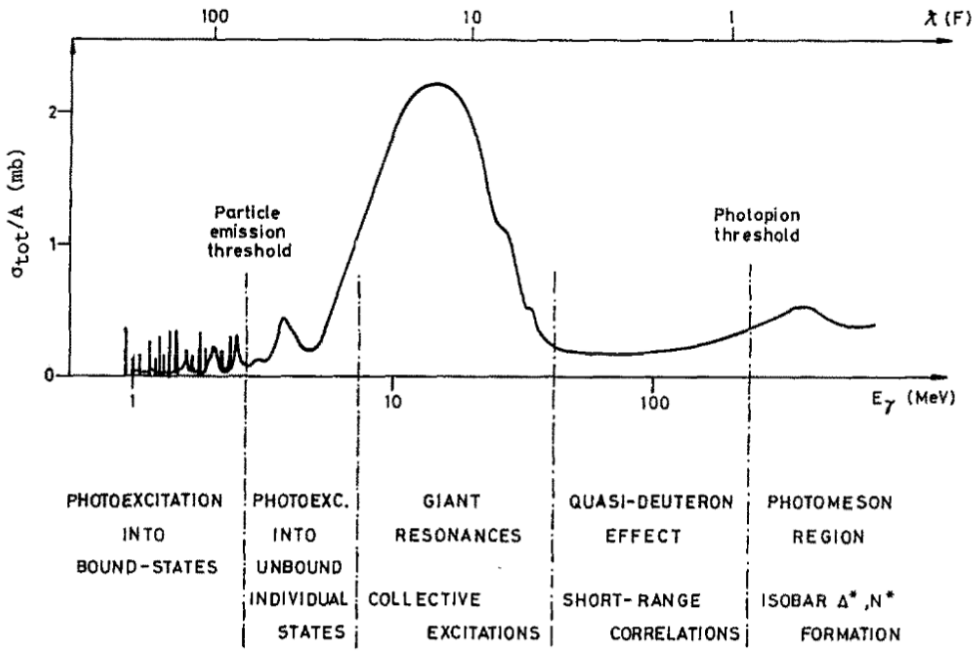


Figure 1: Schematic representation of the total photonuclear cross-section per nucleon at low energy. The picture was taken from [8].

### 2.3 Cross-section evaluation

There are two ways to evaluate a photonuclear cross-section on an isotope, based on experimental data. The first one is connected with the systematic study of all of the experimental cross-section data available for the relevant isotope target. In these cases, a thorough analysis of any experimental data discrepancies in shape, absolute values, and average energies is required. These discrepancies can be connected with the calibration of photon energies, absolute cross-section normalization, or differences in photon spectra. The elimination of these discrepancies for the evaluated cross-section can be done by reducing experimental data to quasi-monoenergetic photon spectrum and subsequent removal of the systematic discrepancies by different cross-section normalization and energy shifts due to calibration. This approach was implemented by the CDFE laboratory [5].

The second approach to cross-section evaluation is connected with previously defined GDR and QD models. In this case, total photo-absorption cross-section is defined by the sum of two components [7]:

$$\sigma_{tot}(E_\gamma) = \sigma_{gdr}(E_\gamma) + \sigma_{qd}(E_\gamma) \tag{5}$$

After the initial model based on theoretical prediction is evaluated the comparison has to be done between available experimental data and model total absorption cross-section or, more commonly, with subsequent nuclear reaction calculations. The subsequent reaction can be presented by emission spectra, angular distribution, or different excitation functions, which show the dependence of the yield of a reaction channel from the excitation energy of the compound nucleus. The examples of such function can be the following reactions - ($\gamma$,1n), ($\gamma$,1p), ($\gamma$,2n), ($\gamma$,2p), etc. If the calculated subsequent nuclear reactions disagree with the measured value adjustment of the input model parameters is made to optimize agreement between calculation and experiment. For heavy nuclei, it is also important to take into account the photofission process. To get photofission probability one has to calculate fission transition coefficients and take into account spin and parity of the transition state [13].

The cross-section evaluation based on two approaches mentioned above was made by International Atomic Energy Agency(IAEA). A relatively complete photo-nuclear data files in ENDF format for 219 isotopes become available in August 2020. A selection of the worldwide experimental measurement has been accurately performed to provide to the scientific community photonuclear data at $5 - 140\ MeV$ energy region [7]. That cross-section evaluation database was used to develop low energy region of the new photonuclear cross-section model at the Geant4 toolkit.

## 3 New photonuclear model

The GEANT4 is a toolkit for the simulation of the passage of particles through matter. Its functionality includes event generation, particle tracking, visualization, geometry descriptions, and physics models. It is used in various applications, such as high-energy physics experiments, astrophysics, radiation protection, medical physics, etc [14–16].

### 3.1 Model database

The data for the new model is taken from the IAEA evaluated photonuclear data library (IAEA/PD-2019) [17]. The evaluations have been contributed from five different collaborations assembled under an international coordinated research project (CRP) [18]. Details of the experimental and evaluation efforts in this CRP are explained in this publication [7]. IAEA data library consists of 219 isotopes in ENDFL-6 format type, however different ENDF-6 data format representations have been used by different evaluators for the energy below 140 MeV. As a result, the IAEA photonuclear library contains six slightly different types of ENDFL-6 data files. The documentation with the format description and verification procedure can be found at the official IAEA site at nuclear data services [19]. According to these format descriptions, the cross-section data was taken for every isotope in the database. The results were compared for all six format types with the initial database plots, that were made by CRP, and located at IAEA database along with ENDL-6 files [17]. The example of this comparison is presented in Figure 2.

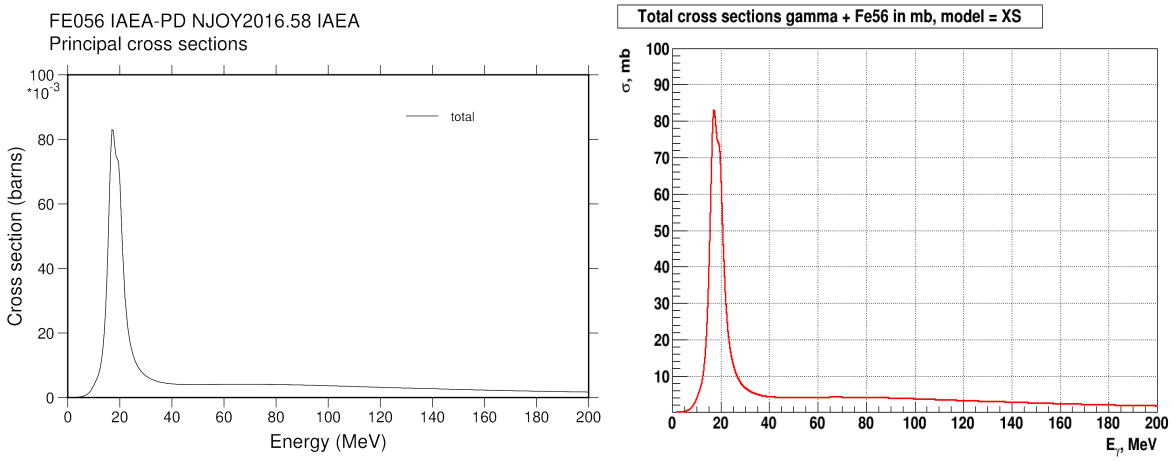


(a) IAEA data cross-section. The picture is from [17].

(b) Retrieved data

Figure 2: Comparison of IAEA evaluated data with the data retrieved for $^{56}$Fe from ENDFL-6 format files [19].

Additions were made to the initial IAEA isotope cross-section data: point with 0 cross-section value added to the left boundary to describe energies lower than evaluated data. Then the following algorithm was applied to create a new Geant4 database with files with an energy range from 0 to 130 MeV for every element with a number of protons Z from 1 to 94 and all available isotopes :

1. All available isotope data is copied to the final model database. Low energy points with zero value and high energy data points above 130 MeV are truncated. In this case, parametrization is non-linear and remains the same as in initial IAEA data files. The data extraction and interpolation are made with G4PhysicsFreeVector. There is no need to optimize isotope database initialization due to more rare usage of isotope cross-section in a run time of the simulation.
2. For element cross-section file an energy step is calculated from IAEA photonuclear data, by finding the minimum energy value between two consecutive cross-section points for all element isotopes. The data are stored in G4PhysicsLinearVector container for most number of elements. This way it is possible to accurately describe resonance with constant energy step, not lose any initial IAEA data and make initialization of the database faster, with the fewest possible cross-section data points.
3. For elements without any relevant isotope data files, or if the total abundance of all presented at IAEA database isotopes has a substantially low value the cross-section data on the element were taken from the previous Geant4 photonuclear CHiral Invariant Phase Space (CHIPS) model [14–16]. In this case, linear parametrization of a cross-section is used with the fixed energy step value - 0.5 MeV. The further interpolation is made by the existing Geant4 class - G4PhysicsLinearVector [14]. The threshold for the isotope sufficient total abundance was put as 1.1 $\%$. This procedure was applied for the following elements - He, B, Ne, P, Ga, Br, Kr, Rb, Tc, Pm, Yb, Ir, Hg, Tl, Po, At, Rn, Fr, Ac, Pa.
4. In case of only one isotope file with the abundance higher than indicated previously threshold, this cross-section on isotope was copied as element cross-section to the model database. Mostly in this case linear cross-section parametrization is used with the step value calculated from item 2 and G4PhysicsLinearVector interpolation method. But for some cases, the step value is too small. Therefore to not exaggerate the size of the database, some exceptions were made. If the calculated step value is lower than 0.1 MeV then the initial IAEA file with unequal energy step between cross-section data points is copied to the final model database. In the case of this non-linear parametrization, G4PhysicsFreeVector is used to further retrieve and interpolate data. The complete list of such exceptions - Be, C, N, O, Co, Y, Rh, Tb, Ho, Tm, Ta.
5. If applicable, all available isotope cross-section IAEA data is retrieved and interpolated. In addition, the sum of abundance for all retrieved isotope data files is calculated. Afterwards at each energy point $E_i$ element cross-section is calculated:

$$\sigma_{element}(E_i) = \frac{\sum_{j=1}^{N} \sigma_j(E_i) * X_j}{\sum_{j=1}^{N} X_j} \,, \tag{6}$$

   where $N$ is the number of available isotopes, $\sigma_j$ and $X_j$ is a cross-section and an abundance of isotope $j$ respectively.

For hydrogen the procession algorithms were different because there is no GDR and QDR possible in a photon-proton collision. Therefore for hydrogen photo-absorption cross-section there is a threshold around delta resonance region ($E_\gamma \backsim 140 MeV$ ). However, for faster initialization, a cross-section of every element must be presented in the model database. Consequently for H special file was created with two data points with zero cross-section value: one at 0 MeV the other one at 130 MeV.

The code that was developed to process initial ENDFL-6 data files and convert them to the final version of the model database is uploaded to the Geant4 testing suite repository repository along with updated photonuclear cross-section HadrHN unit test.

### 3.2 New photonuclear cross-section

The purpose of this work is to add to Geant4 new more accurate photonuclear cross-section class G4GammaNuclearXS which inherits from G4VCrossSectionDataSet interface [14–16]. G4GammaNuc-

learXS is a base class for gamma-nuclear cross-section based on data files from IAEA Evaluated Photonuclear Data Library [17] on the energy region between 0-130 MeV. The data was retrieved and interpolated from model database files with either G4PhysicsLinearVector or G4PhysicsFreeVector Geant4 vector containers [14]. To describe delta resonance and photo-meson energy region at Geant4 new photonuclear model, the linear connection with the previously implemented Geant4 CHIPS model was added for energies between 130-150 MeV. The CHIPS model is implemented at the G4PhotoNuclearCrossSection cross-section class which also inherits from the G4VCrossSectionDataSet interface and provides the total inelastic cross-section for photon interactions with nuclei. The CHIPS cross-section is a parameterization of data that covers all incident gamma energies. Comparison with the CHIPS at low energies is showed for $^{208}$Pb at Figure 3. In some cases, a new model can describe excitation of nuclear levels which take place at energies lower than GDR energy as shown in Figure A.1. Admittedly such description of nuclear structures is not always the case as shown in Figure A.2. Nuclear structure description existence depends on initial IAEA evaluation data files. Data points were taken from EXFOR web database retrieval system [20]. Additional graphs for other isotopes can be found in Appendix A.1. Systematic uncertainties of data are compatible with the size of small peaks in Fig. A.2 or Fig.3.

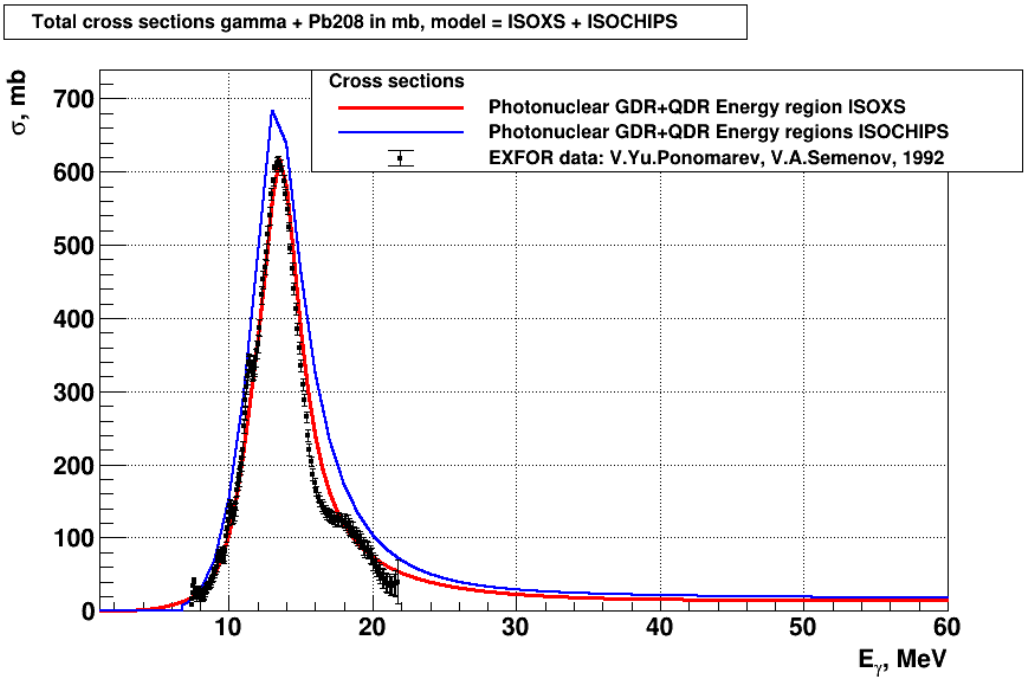


Figure 3: Total photonuclear cross-section from the new model (ISOXS) and old Geant4 photonuclear model(ISOCHIPS) for GDR energy region for $^{208}$Pb versus EXFOR data.

For some rare isotopes, there is no evaluated cross-section data in IAEA photonuclear data library. If such data is requested by the user through new photonuclear class G4GammaNuclearXS methods, then cross-section will be calculated in the following way:

$$\sigma_{isotope(E_\gamma)} = \frac{\sigma_{element}(E_\gamma) * A_{isotope}}{\sum_{j=1}^{N} A_j * X_j}\ , \tag{7}$$

where $A_j$ and $X_j$ are atomic mass and abundance of isotope $j$ respectively, $\sigma_{element}$ is the cross-section of the corresponding chemical element. Undoubtedly this is a very rough approximation of the true photoabsorption cross-section, but without reliable evaluation data, there are two options for the new model in this case. That is to return 0 cross-section value or return order of magnitude cross-section estimation. As a result, the approach represented by equation (7) was implemented.

### 3.3 Delta resonance and photo-meson energy regions

Example of new photonuclear class cross-section output for higher energy range is presented at Figure 4. The previous Geant4 photonuclear model had a problem with high energy connection that can be seen at isotopes of hydrogen and helium. This issue was fixed by connection with element cross-section at energies $\backsim$ 10 GeV. The comparison with the CHIPS model for deuterium is showed in Figure 5. Additional graphs with evaluated photo-nuclear cross-sections can be found in Appendix A.2.

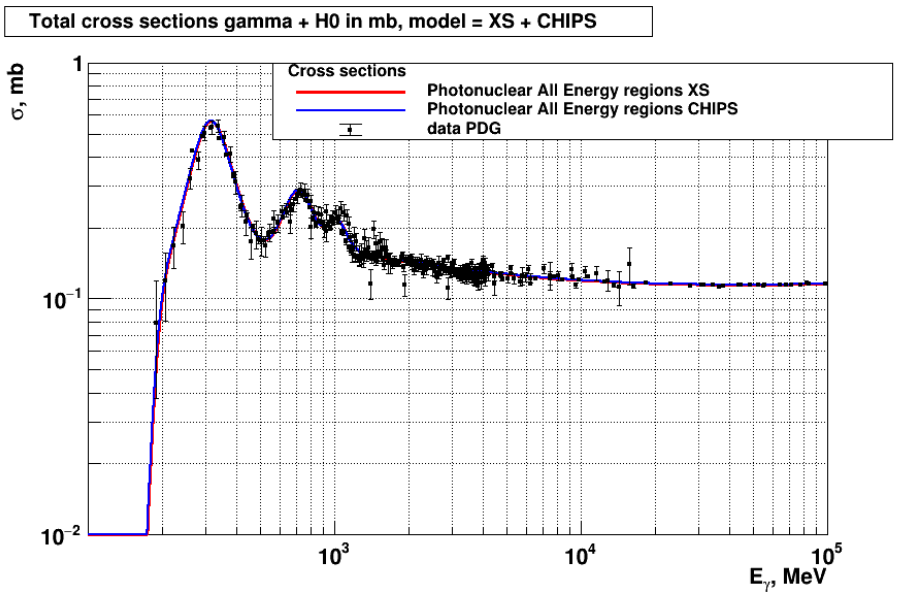


Figure 4: Total photonuclear cross-section from the new model (XS) and old Geant4 photonuclear model (CHIPS) for a broad energy range for hydrogen versus PDG data [1].

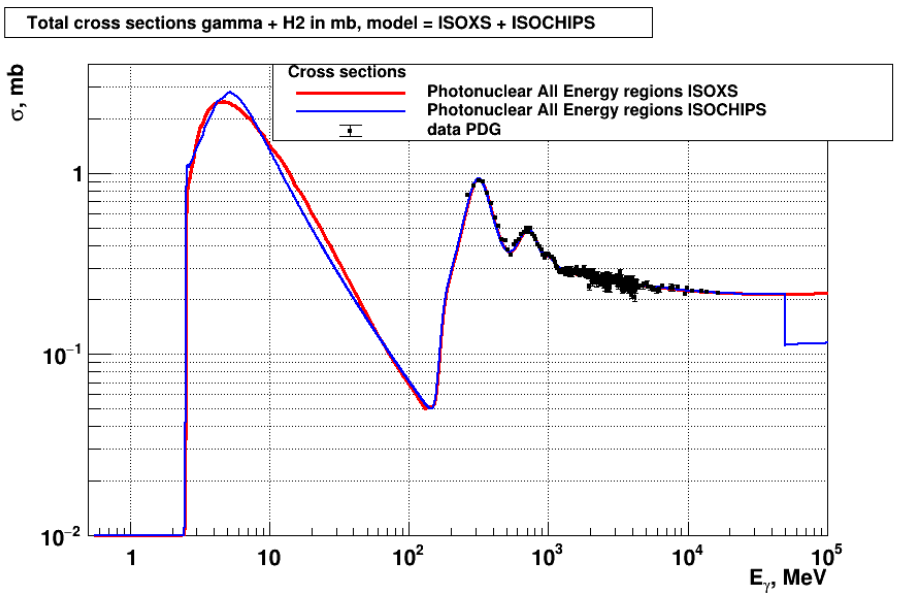


Figure 5: Total photonuclear cross-section from the new model (ISOXS) and old Geant4 photonuclear model(ISOCHIPS) for a broad energy range for deuteron versus PDG data [1].

## 4 Conclusions

New photonuclear cross-section model G4GammaNuclearXS is implemented for Geant4, the source code for the new class will be freely available with Geant4 version 11.0 at December 2021 in *Geant4/source/processes/hadronic/cross_sections/*. A new photonuclear database founded on IAEA photonuclear data library is included in G4PARTICLEXS 4.0 dataset. The algorithm of the database creation was described and code provided in the new application HadrHN-IAEA. Existing at Geant4 unit test HadrHN were modified for verification of the new photonuclear model.

The cross-sections provided by the new class were compared with cross-sections of previously implemented CHIPS photonuclear model and experimental data. It was shown that the new model cross-sections have some discrepancies with available experimental data especially around the right slope of GDR. Moreover, the new model in most cases does not describe excitation of nuclear levels which take place at energies lower than GDR energy, because the data is not available. This low energy process does not produce neutrons but provides re-scattering of a photon. However, the new model more precisely describes giant dipole resonance than the CHIPS model for the majority of elements, and cross-section at high energies for isotopes of helium and hydrogen is fixed. So this new cross-section may be recommended for any Geant4 applications.

## Acknowledgements

We thank CERN Summer Student Programme for providing this great opportunity to perform this study. I am also grateful to my supervisor for the clear guidance and helpful suggestions every step of the way going through with this interesting project.

## Bibliography


[1] Smoot, George Fitzgerald. "Review of particle physics. Passage of particles through matter" Progress of Theoretical and Experimental Physics (2020).

[2] O. V. Bogdankevich and F. A. Nikolaev, Methods in Bremsstrahlung Research. New York, USA: Academic Press (1966).

[3] A. Tzara, “A method of producing a narrow spectrum of high-energy photons”, Comptes Rendus Acad. Sci.56 (1957).

[4] H. Ohgaki, H. Toyokawa, K. Kudo, N. Takeda, andT. Yamazaki, “Generation and application of laser-Compton gamma-ray at ETL”, Nucl. Inst. Meth. A455, 54 (2000).

[5] V.V.Varlamov, B.S.Ishkhanov, V.N.Orlin, and S. Y. Troshchiev, “New data for 197Au ($\gamma$,nx) and 197Au ($\gamma$,2nx) reaction cross sections”, Bull. Rus. Acad. Sci.74 (2010).

[6] V.V. Varlamov, V. V., Efimkin, N. G., Stepanov, M. E. (1996). Photonuclear data: analysis of discrepancies and evaluation (No. JAERI-CONF–96-008).

[7] Kawano, T., Cho, Y. S., Dimitriou, P., Filipescu, D., Iwamoto, N., Plujko, V., ... 'I&' Wiedeking, M. (2020). IAEA photonuclear data library 2019. Nuclear Data Sheets, 163, 109-162.

[8] Findlay, D. J. S. "Applications of photonuclear reactions." Nuclear Instruments and Methods in Physics Research Section B: Beam Interactions with Materials and Atoms 50.1-4 (1990): 314-320.

[9] Goldhaber, M., Teller, E. (1948). On nuclear dipole vibrations. Physical Review, 74(9), 1046.

[10] S. C. Fultz, R. L. Bramblett, J. T. Caldwell, and N. A. Kerr, “Photoneutron cross-section measurements on gold using nearly monochromatic photons,” Phys.Rev.127, 1273 (1962).

[11] V. A. Plujko, O. M. Gorbachenko, R. Capote, and P. Dimitriou, “Giant dipole resonance parameters of ground-state photoabsorption: Experimental values with uncertainties,” At. Data Nucl. Data Tables123–124, 1 (2018).

[12] M. B. Chadwick, P. Oblozinsk, P. E. Hodgson, and G. Reffo, “Pauli-blocking in the quasideuteron model of photoabsorption,” Phys.Rev.C44, 814 (1991).

[13] Strutinsky, V. M. (1967). Shell effects in nuclear masses and deformation energies. Nuclear Physics A, 95(2), 420-442.

[14] Agostinelli, Sea, et al. "GEANT4—a simulation toolkit." Nuclear instruments and methods in physics research section A: Accelerators, Spectrometers, Detectors and Associated Equipment 506.3 (2003): 250-303. `https://geant4.web.cern.ch`.

[15] Allison, John, et al. "Geant4 developments and applications." IEEE Transactions on nuclear science 53.1 (2006): 270-278.

[16] Allison, J., et al. "Recent developments in Geant4." Nuclear Instruments and Methods in Physics Research Section A: Accelerators, Spectrometers, Detectors and Associated Equipment 835 (2016): 186-225.

[17] IAEA Evaluated Photonuclear Data Library (IAEA/PD-2019) `https://www-nds.iaea.org/photonuclear`.

[18] M. Wiedekin, D. Filipescu, and P. Dimitriou. Updating photonuclear data library and generating a reference database for photon strength functions. IAEA Report INDC(NDS)-0777, IAEA, Vienna, 2019.

[19] H. Kawada, J.-C. Sublet, S. Okumura and T. Kawano. Processing of the Evaluated Photonuclear Data Library (IAEA/PD-2019) `https://www-nds.iaea.org/publications/nds/iaea-nds-0232/`.

[20] Otuka, N., et al. "Towards a more complete and accurate experimental nuclear reaction data library (EXFOR): international collaboration between nuclear reaction data centres (NRDC)." Nuclear Data Sheets 120 (2014): 272-276. `https://www-nds.iaea.org/exfor/`

# Appendix

## A Additional plots

### A.1 GDR and QD energy region

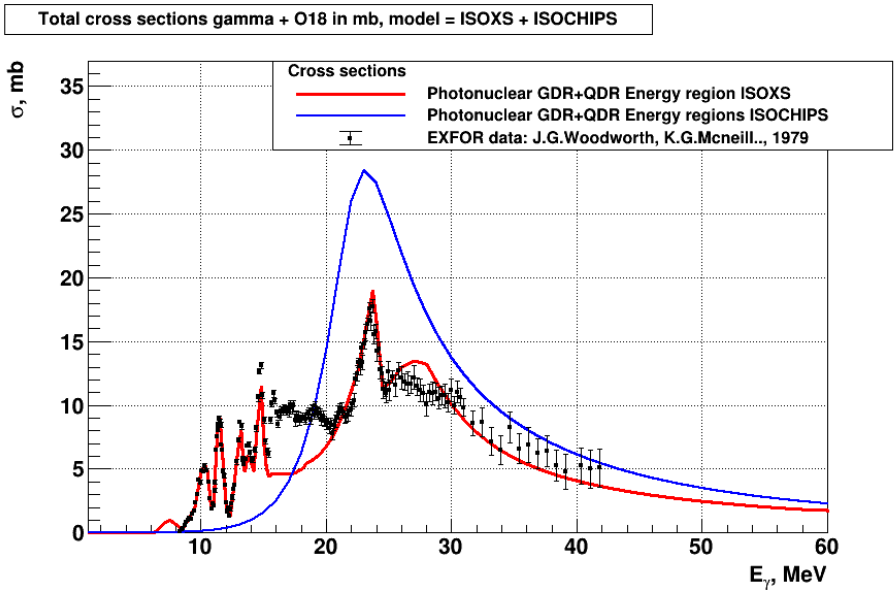


Figure A.1: Total photonuclear cross-section comparison between new (ISOXS) and old (ISOCHIPS) Geant4 photonucelar models for $^{18}$O versus EXFOR data.

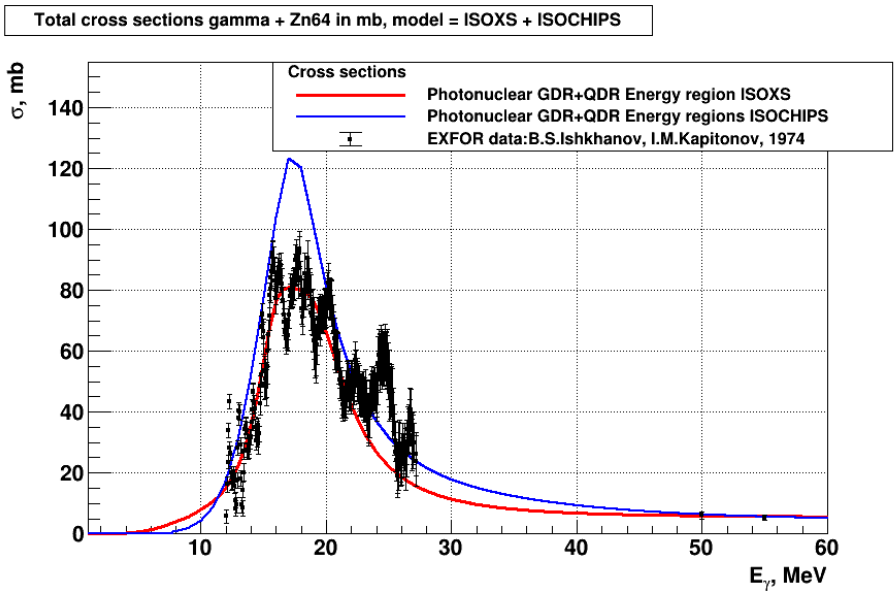


Figure A.2: Total photonuclear cross-section comparison between new (ISOXS) and old (ISOCHIPS) Geant4 photonucelar models for $^{64}$Zn versus EXFOR data.

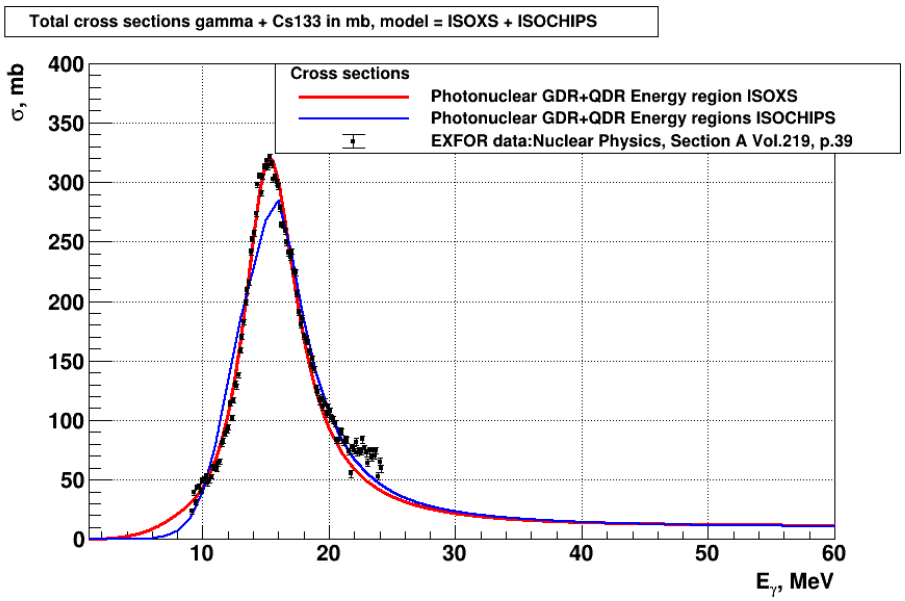


Figure A.3: Total photonuclear cross-section comparison between new (ISOXS) and old (ISOCHIPS) Geant4 photonucelar models for $^{133}$Cs versus EXFOR data.

## A.2 Delta resonance and photo-meson energy regions

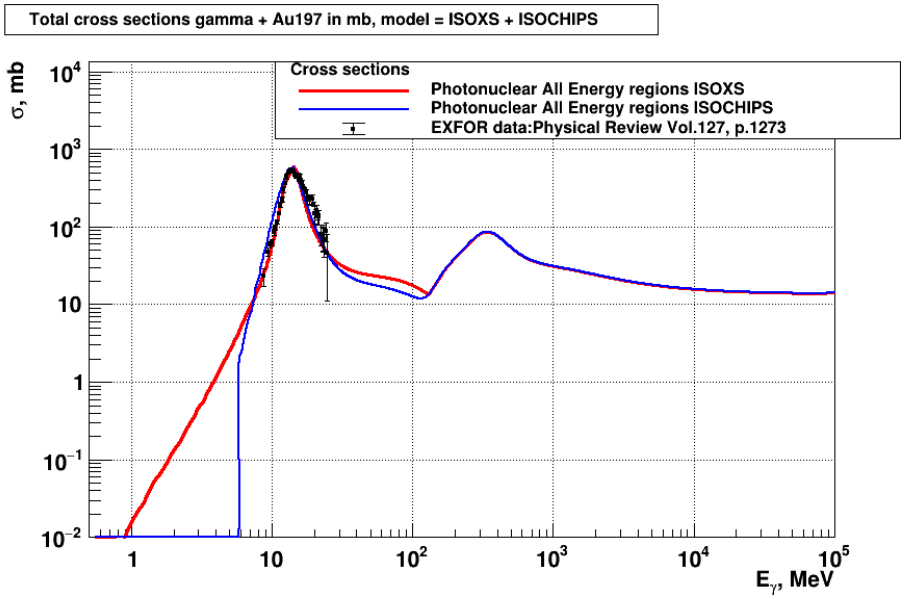


Figure A.4: Total photonuclear cross-section comparison between new (ISOXS) and old (ISOCHIPS) Geant4 photonucelar models for $^{197}$Au versus EXFOR data.

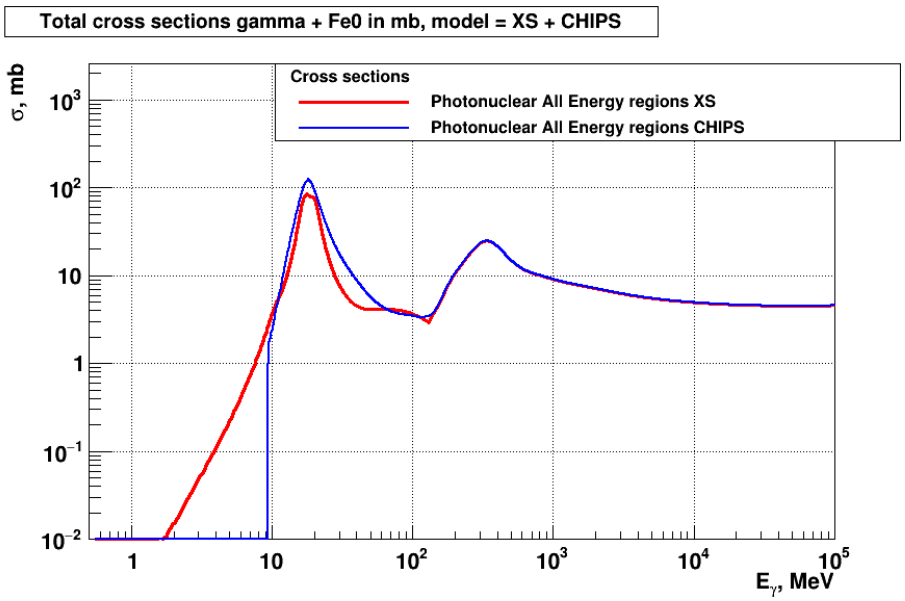


Figure A.5: Total photonuclear cross-section comparison between new (XS) and old (CHIPS) Geant4 photonucelar models for iron versus EXFOR data.

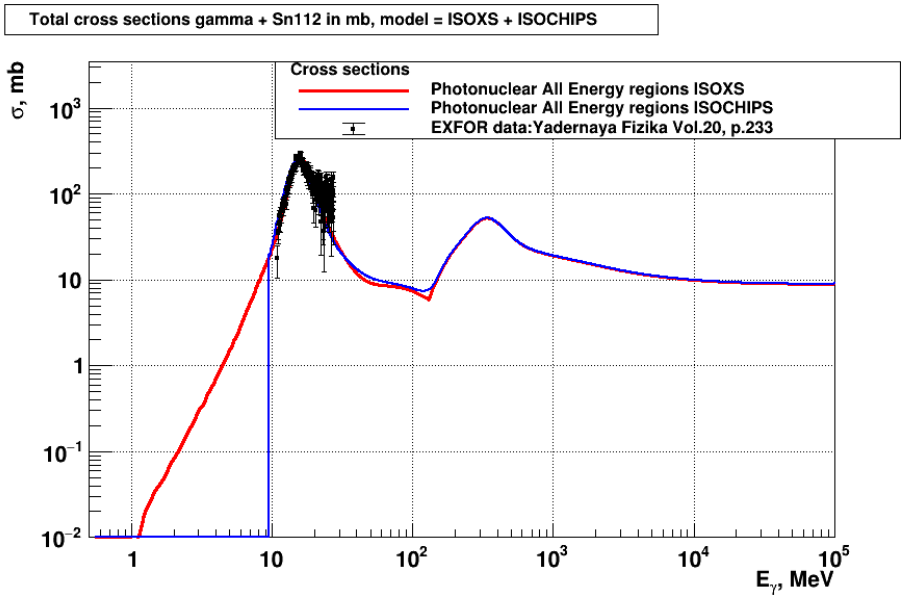


Figure A.6: Total photonuclear cross-section comparison between new (ISOXS) and old (ISOCHIPS) Geant4 photonucelar models for $^{112}$Sn versus EXFOR data.

### A.3 Broad energy range

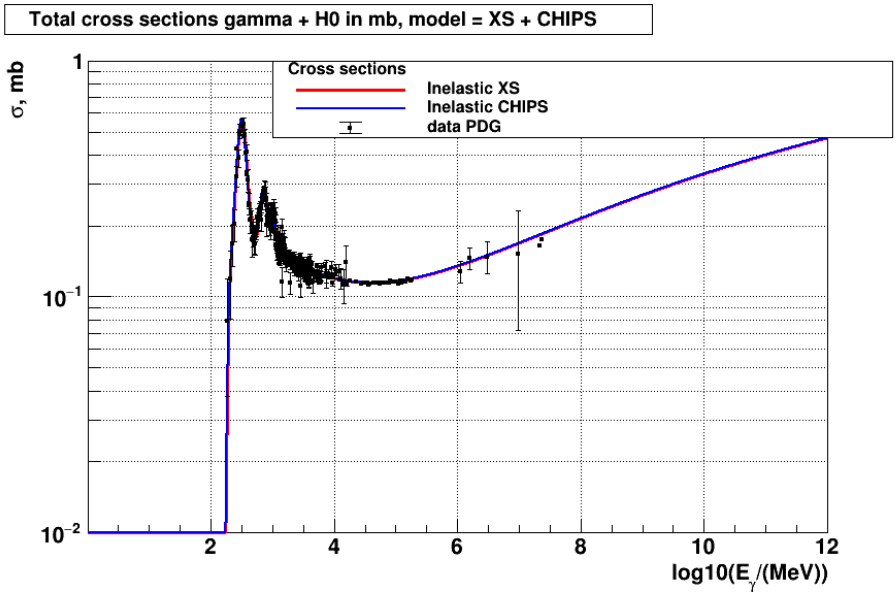


Figure A.7: Total photonuclear cross-section comparison between new (XS) and old (CHIPS) Geant4 photonucelar models for hydrogen versus EXFOR data.

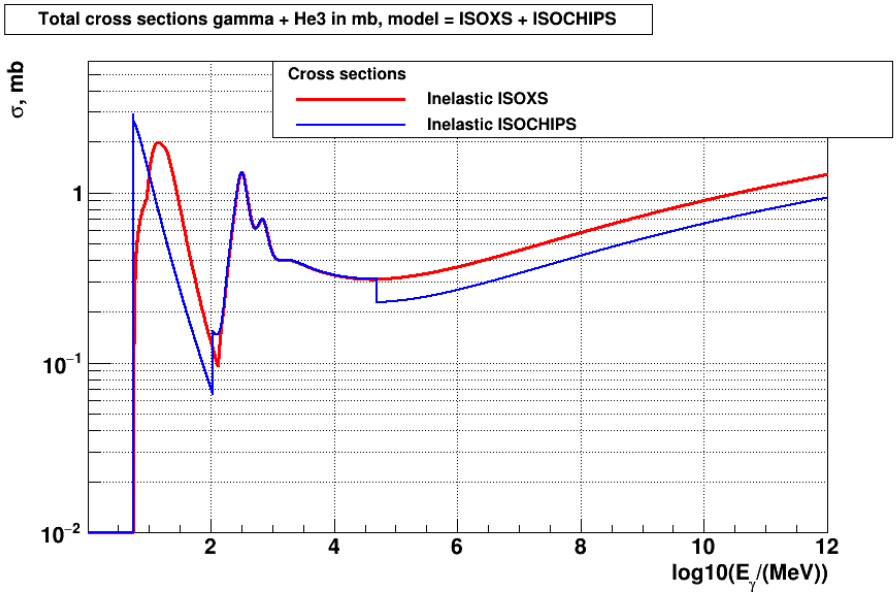


Figure A.8: Total photonuclear cross-section comparison between new (ISOXS) and old (ISOCHIPS) Geant4 photonucelar models for $^3$He versus EXFOR data.